Structure and Properties of Regenerated Cellulose Films Coated with Polyurethane–Nitrolignin Graft-IPNs Coating

Jin Huang, Lina Zhang

Department of Chemistry, Wuhan University, Wuhan 430072, People's Republic of China

ABSTRACT: A regenerated cellulose film (RC) was coated with a graft-IPNs coating, which was composed of castor oil-based polyurethane and 2.8 wt % nitrolignin (NL), to obtain water-resistant films. The effects of NCO/OH molar ratio and different polyols, such as 1,4-butanediol (BDO) and trimethanol propane (TMP), on the structure and properties of the coated RC films were investigated. With an increase of the NCO/OH molar ratio, the tensile strength of the coated films increased, but the water resistivity and size contraction hardly changed. The coated films with TMP exhibited the higher breaking elongation at 1.5 of the NCO/OH molar ratio, while those with BDO have more excellent tensile strength, water resistivity, and dimensional stability. The coated films with the graft-IPNs coating exhibited superior water resistivity and dimensional stability. The light transmittance of the coated films was more excellent than that of the RC film. Moreover, the results from the IR and electron probe microanalysis (EPMA) showed that the chemical bonding occurred between cellulose and coating, and the introduction of NL plays an important role in the enhancement of the interface adhesion of the coated films. Atomic force microscopy (AFM) depicted the flat and dense surface of the coated films, which restricted the water vapor penetration and the size contraction, resulting in the enhancement of water resistivity. © 2002 Wiley Periodicals, Inc. J Appl Polym Sci 86: 1799–1806, 2002

Key words: cellulose; graft-IPN; lignin; polyurethane

INTRODUCTION

The research and application of cellulose, the most abundant natural polymer, have drawn more and more attention. Therefore, the development of cellulose has become an important task in the 21st century due to the its renewable, biodegradable, biocompatible, and derivatizable characteristics, which is the basis of manufacturing functional materials to meet diverse needs and a potential substitution for some petrochemical materials to prevent the environment from pollution and disposal to obtain great commercial value.[1,2] The application of the cellulose products is limited because of the sensibility of cellulose to water. Many research groups have managed to apply the technique of coating, a simple and fast method, to improve the water resistivity, and the available water-resistant coating, such as chitosan/cellulose powder coating,[3] polylactic acid, and its derivatives[4] and nitrocellulose coating,[5] were developed. However, these coatings cannot meet the practical need, for example,

the nitrocellulose coating layer was easily peeled from the regenerated cellulose film after soaking in the water for 5 min.

Interpenetrating polymer networks (IPNs) is a special class of polymer blend involvs crosslinked polymers, which can promote the miscibility between component polymers, and is evaluated as an effective means to modify the properties to meet specific demands. In our laboratory, IPNs coatings from castor oil-based polyurethane (PU)/nitrocellulose,[6] PU/nitrochitosan,[7] and PU/elaeostearin[8] have been satisfactorily used to enhance the water-resistible ability of regenerated cellulose films. These coated cellulose films exhibit excellent tensile strength, water resistivity, and optical transmission, and particularly biodegradability.[9] It is well known that the adhesion between the coating layer and the film plays an important role in the improvement of the mechanical properties and water resistivity of the material. The condition of a good adhesion mainly depends on an intimate contact between the solids to be joined, which usually results from the interdifussion of the polyurethane prepolymer molecules into the interfacial layers. IPNs coatings derived from polyurethane and other polymer exhibits the good adhesive ability due to the reaction of the excessive —NCO with —OH of cellulose, resulting in the formation of a shared PU network crosslinked simultaneously with the IPNs coating and RC film in the adhesive interface.[10] Moreover, IPNs coating favors the enhancement of properties for

the coated RC films and accelerate the curing process, compared with pure polyurethane.

In our previous work,[11–13] a series of PU/nitrolignin (UL) coating with excellent mechanical properties and thermal stability was satisfactorily synthesized. Moreover, the analysis on morphology and structure of the coating indicated that nitrolignin (NL) was grafted on PU to form the graft-IPNs structure.[13] It is beneficial to make use of this coating for the improvement and optimization of properties of regenerated cellulose (RC) films. In this work, the effects of polyols with a different amount of —OH and NCO/OH molar ratio in the coatings on the interfacial adhesion and properties of the coated films were studied. The morphology and structure of the surface for the coated films were observed by atomic force microscopy (AFM) and Fourier transform infrared spectroscopy (FTIR), while the interfacial properties was investigated by electron probe microanalyzer (EPMA). The mechanical, thermal, optical, and other properties of the coated films were measured, and the structure–properties relationships were discussed.

EXPERIMENTAL

Materials

All the chemical regents were obtained from commercial resources in China. The cotton linter was purchased from Hubei Chemical Fiber Group Ltd of China, and its viscosity-average molecular weight (M_η) was determined in cadoxen at 25°C by viscometer to be 10×10^4. Alkali lignin from bamboo was supplied by Guangzhou Chemistry Institute of China. Castor oil, chemical pure, was dehydrated at 100°C under 20 mmHg for 1 h. 2,4-Tolylene diisocyanate (TDI) was redistilled before use. 1,4-Butanediol (BDO) from the Medicine Group of Shanghai in China, and trimethanol propane (TMP) from First Chemical Reagent Factory of Shanghai in China were used as a chain-extender and crosslinker, respectively.

Synthesis of polyurethane–nitrolignin coatings

The nitrolignin (NL) was prepared and characterized to be N content 8.08%, and its weight-average molecular weight (M_w) was determined to be 19.2×10^4 according to the former method.[11] To a round-bottom flask with TDI, castor oil was slowly added with stirring. The reaction was carried out at 45°C for 50 min to obtain PU prepolymer. The NCO/OH molar ratio of PU prepolymer was calculated to be 2.0 by the equivalent weights per —OH mol of castor oil (345 g) and of TDI per —NCO mol (87 g). The compositions of the PU and UL coatings with different NCO/OH molar ratios are listed in Table I. The UL coatings were obtained from the mixture of PU prepolymer/THF

TABLE I
Compositions of Polyurethane–Nitroligin System Containing 2.8 wt % NL and 3.0 g PU Prepolymer with NCO/OH Molar Ratio 2.0

Sample	Polyol BDO/mol	TMP/mol	NCO/OH molar ratio
UL-0	—	—	2.0
UL-B1	0.0006	—	1.8
UL-B2	0.0019	—	1.5
UL-B3	0.0038	—	1.2
UL-B4	0.0052	—	1.05
UL-T1	—	0.0006	1.8
UL-T2	—	0.0019	1.5
UL-T3	—	0.0038	1.2
UL-T4	—	0.0052	1.05

The coatings of PU series have the corresponding compositions except for the addition of NL.

solution, NL/THF solution and BDO/THF or TMP/THF solution, then stirred for 0.5 h under room temperature. The PU coatings were prepared similar to the above method except for adding NL/THF solution. According the compositions of every coating, UL coatings were coded as UL-0 (without polyol), UL-B1 ~ UL-B4 (containing BDO), or UL-T1 ~ UL-T4 (containing TMP), while PU coatings with the corresponding polyols were coded as PU-B1 ~ PU-B4 or PU-T1 ~ PU-T4. The solid content of all UL and PU coatings were about 18%. It is worth noting that the curing process of the coatings containing NL was obviously faster than that of the coatings without NL.

Preparation of coated films

The cotton linter was dissolved in 6 wt % NaOH/5 wt % thiourea aqueous solution, followed by freezing in a refrigerator under −5°C for 12 h. The freezing solution of cellulose was unfrozen in ice water for 6 h, then we obtained a transparent solution by ultracentrifugal. According to our method,[14] the cellulose solution was spread over a glass plate, and then coagulated in with 5 wt % $CaCl_2$ and 3 wt % HCl solutions for 3 min, respectively, to obtain the regenerated cellulose (RC) films.

The coatings mentioned above were coated on the both sides of the RC films. The coated RC films were placed in the air for 0.5 h, and then cured under 35 ± 2°C for 4 h. The RC films coated with UL coatings were coded as CL-0, CL-B1 ~ CL-B4 (containing BDO) or CL-T1 ~ CL-T4 (containing TMP), while those coated with PU coatings coded as CU-0, CU-B1 ~ CU-B4, or CU-T1 ~ CU-T4. The content of coatings in two sides of the coated films were calculated to be the mean value of 28% by the weighing method.

Characterization of coated films

FTIR spectra of coated films and RC film were performed by taking the KBr method on an FTIR Spec-

trometer (Spectrum One, Perkin-Elmer Instruments, Norwalk, CT).

AFM images for the surface of the coated films and RC film were carried out in the contact mode with a commercial instrument (Picoscan Molecular Imaging, USA). Electron probe microanalysis (EPMA) was measured by Electron Probe Microanalysis JXA-8800R (JOEL Super-probe, Japan). The elector-conductive film was fixed between two steel sheets, and the one-dimensional distribution of nitrogen element on the cross-section of the coated films was recorded.

Thermogravimetric analysis (TGA) curves of the coated films and RC film were recorded on a WCT-1A thermoanalyzer (Optics Instrument Factory of Beijing, China) under N_2 atmosphere from 20 to 600°C at a heating rate of 10°C min^{-1}.

Tensile strength (σ_b) and breaking elongation (ϵ_b) of the coated films and RC film were measured on a universal testing machine (CMT6503, Shenzhen SANS Test Machine Co. Ltd, China) with the tensile rate of 5 mm min^{-1} according to ISO6239-1986 (E). The water resistivety (R) of the coated films, and RC film was evaluated from the values of $\sigma_{b,wet}$ in the wet state and $\sigma_{b,dry}$ in the dry state:

$$R = \sigma_{b,wet}/\sigma_{b,dry} \qquad (1)$$

The films with 5×5 cm^2 were immersed in water for 24 h, and then naturally dried. The average sizes of the films dried again (d) were measured. The extent of size constriction (Sc) was estimated by:

$$Sc = [(5 - d)/5] \times 100\% \qquad (2)$$

The water vapor permeability (P) of the films was evaluated from the evaporation amount of the water in a beaker (100 mL), which was sealed by the tested films, at 12.5 ± 2°C and 75% relative humidity for 10 days. The values were obtained by:

$$P = (W_0 - W_t)/10S \qquad (3)$$

where W_0 and W_t are the initial and final total weight (g) of the beaker, respectively. S is the effective covered area (cm^2) of the films used.

The percent light transmittance (Tr) of the films in the wavelength range of 200 ~ 800 nm was measured on a UV-160A spectroscope (Shimadzu, Japan).

RESULTS AND DISSCUSSION

Morphology and structure of coated films

FTIR spectra of the films RC, coated films, and corresponding coatings are shown in Figure 1. The coated films exhibited the characteristic absorptions at about 1730 cm^{-1} (C=O stretching), and 1540 cm^{-1}
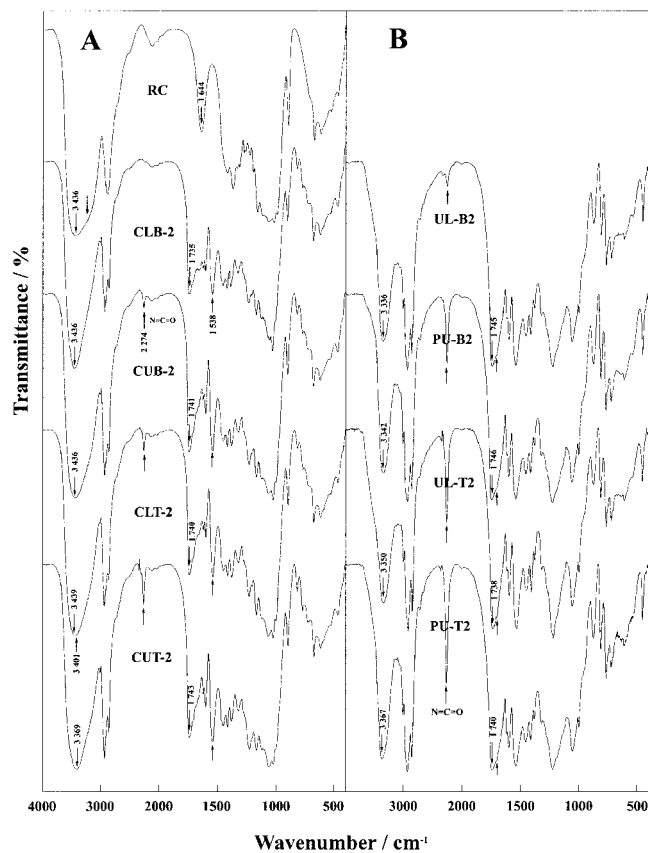

Figure 1 FTIR spectra of RC and the coated films (A), and corresponding coatings (B).

(C—N—H bending) of polyurethane. However, compared with IR spectra of the coatings (B), the peaks at 1642 cm^{-1} (glucose enol form in cellulose) and at 2274 cm^{-1} (free N=C=O groups of PU) for the coated films significantly weakened, indicating that —NCO groups of PU molecules penetrate into cellulose and reacted with —OH groups of cellulose. Interestingly, the intensity of —NCO for the coated films and coatings with NL were obviously lower than that of those without NL, suggesting that —OH of NL reacted with —NCO of PU, and hence accelerated the curing process of the coatings. Moreover, the intensity of —NCO in the coated films were significantly lower than that in corresponding coatings, indicating the occurrence of reaction between —NCO of the coatings and —OH of cellulose. It further proved that the shared PU network formed between the graft-IPNs coating and RC film. Compared with RC film and the coated films without NL, the absorptions at 3400 cm^{-1} of the coated films containing NL became narrow and shifted to high wavenumber, suggesting that the introduction of NL destroyed the hydrogen bonds of polyurethane in the coatings, and even weakened the hydrogen bonds of cellulose when PU molecules in the coating penetrated into the RC film.

The three-dimension (3D) plots of the coated films and RC film observed by AFM were shown in Figure
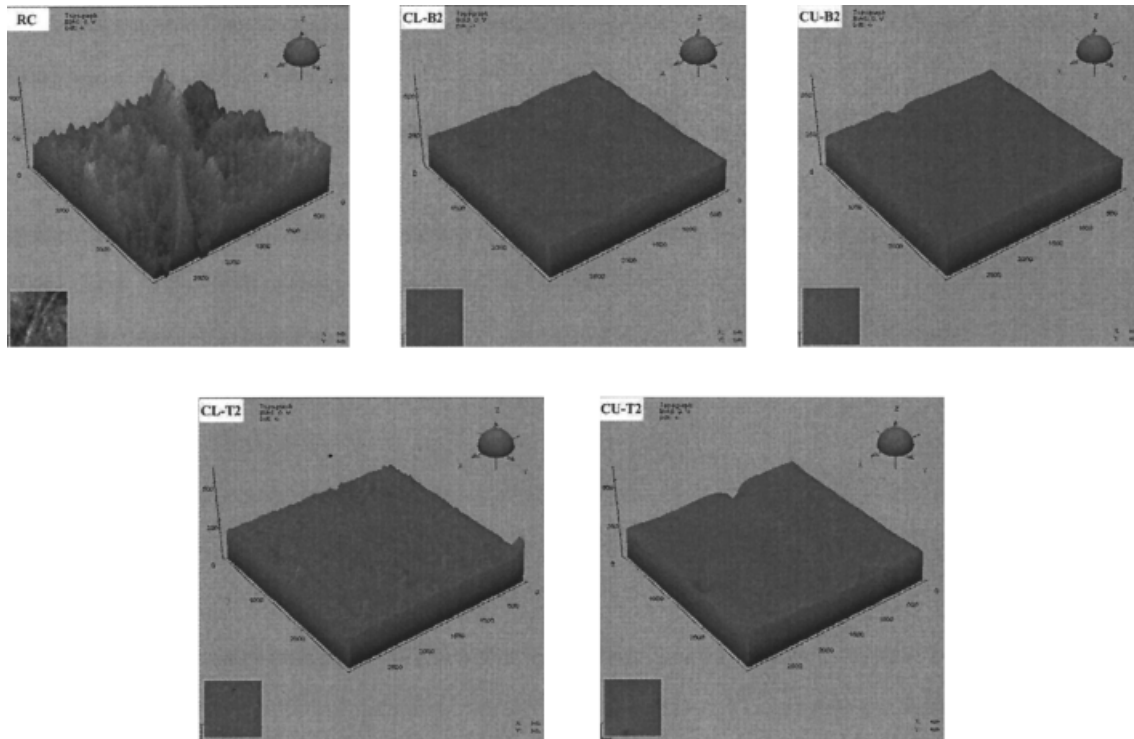
Figure 2 The morphology of surface for RC and coated films by AFM.

2. Compared with the surface of the RC film with porous structure, the coated films showed the flat surface with the dense structure, which was caused by the formation of thin and dense coating layer. Therefore, the water resistivity, size constriction, and water vapor permeability of the coated films were improved. Simultaneously, the coated films containing crosslinker TMP had a slightly rougher surface than those containing chain-extender BDO, suggesting that the steric hindrances of TMP had a detrimental effect on the dense structure of the the coating surface.

Figure 3 shows the one-dimensional distributions of N element on the cross-section of the films CL-B2 and CU-B2 determined by electron probe microanalysis (EPMA). The distribution of N element on the cross-section of CL-B2 is that N content on both sides was higher than in the middle, indicating that UL graft-

IPNs coating penetrated into the front layer of RC films. However, the distribution of N element on the cross-section of CU-B2 exhibited a broad N region, suggesting that the penetration of PU coating into RC film was speedier than that of UL coating. It was noted that the grafted NL in UL coating prevented the diffusion of the PU prepolymer to the RC film. Based on these results, it could be concluded that while forming the grafted IPNs in UL coating, the PU prepolymer molecules simultaneously penetrated into the RC film, in which —NCO reacted with —OH, produce another IPNs. It was considered as a shared network of PU crosslinked with cellulose, and the graft-IPNs coating exists in the N diffusion region of the coated films, resulting a strong interfacial bonding in the coated films.
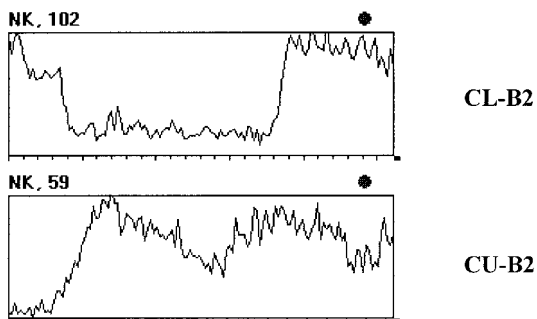
Effects of hard-segment in coating on mechanical properties

Figure 4 shows the varieties of σ_b and ε_b for the coated films and the values of RC film in dry and wet states. The σ_b of the coated films in dry and wet states increased with an increase of NCO/OH molar ratio in coatings, but were correspondingly lower than that of RC film ($\sigma_{b,dry} = 93.26$ MPa, $\sigma_{b,wet} = 15.24$ MPa) except for the coated films with high NCO/OH molar ratio in the wet state. With an increase of the NCO/OH molar ratio, the ε_b of the coated films with BDO in the dry and wet states decreased, and that of the coated films with TMP increased up to 1.5 of the

Figure 3 EPMA on the cross-section of the coated films for the one-dimensional distribution of nitrogen.
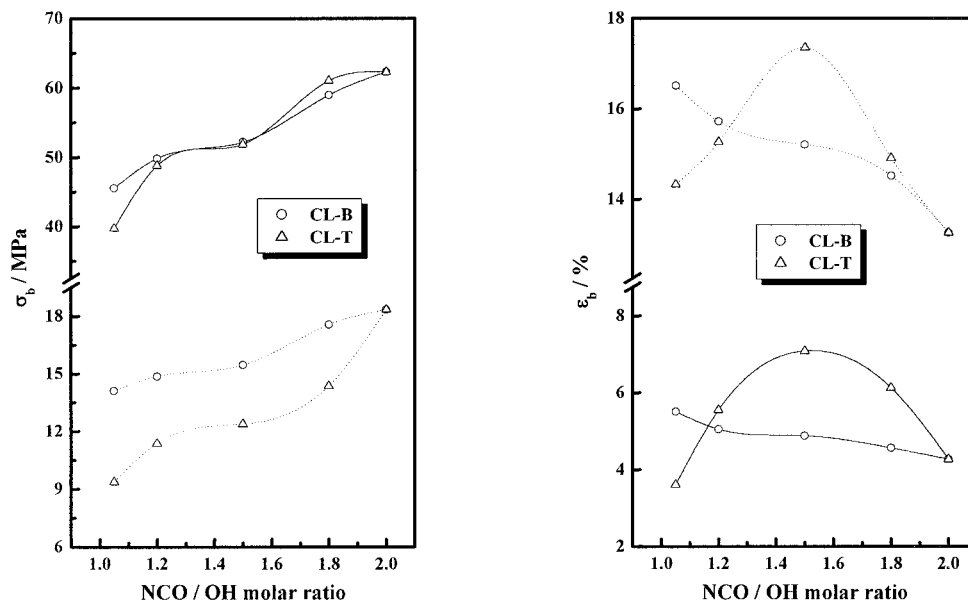
Figure 4 The tensile strength and breaking elongation of the coated films in dry (—) and wet (· · · ·) states.

NCO/OH molar ratio and then decreased. However, all the coated films in the dry or wet state showed higher ε_b values than RC film ($\varepsilon_{b,\mathrm{dry}}$ = 4.20, $\varepsilon_{b,\mathrm{wet}}$ = 8.77). The coated films with BDO exhibited higher σ_b and lower ε_b in the dry and wet states than those of the coated films with TMP except for the ε_b at 1.02 of the NCO/OH molar ratio. The steric hindrance of TMP restricted the formation of shared network, and hence affected the adhesion of interface to result in the inferior mechanical properties.

As shown in Figure 5, the water resistivity (R) of the coated films was significantly enhanced, while the NCO/OH molar ratios have no effect on the R value, but the coated films with BDO exhibited higher R values than those with TMP, resulting from the rela-

tively loose structure of the coated films with TMP, as shown in Figure 2.

Effects of hard-segment in coating on physical properties

The water vapor penetration (P) of the coated films and RC film is shown in Figure 6. It indicated that the coated films exhibited more strong ability to restrict the water vapor penetration than RC film, similar to the results of water resistivity. This was attributed to the hydrophobicity and dense surface of the coating. As shown in Figure 7, the extent of the size contraction (Sc) of the coated films was lower than RC film, suggesting the coating can enhance the dimensional sta-
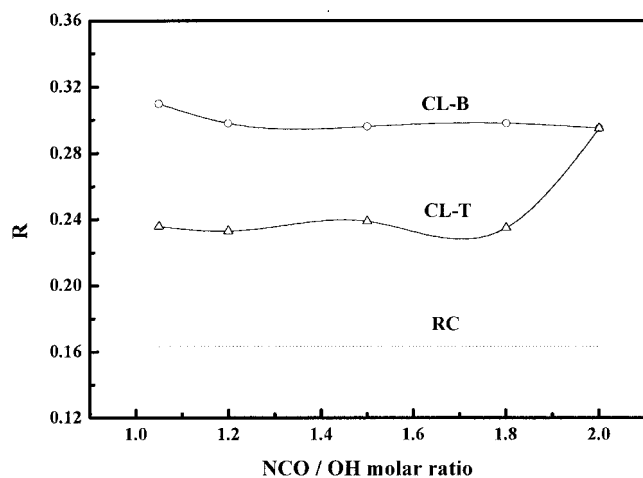

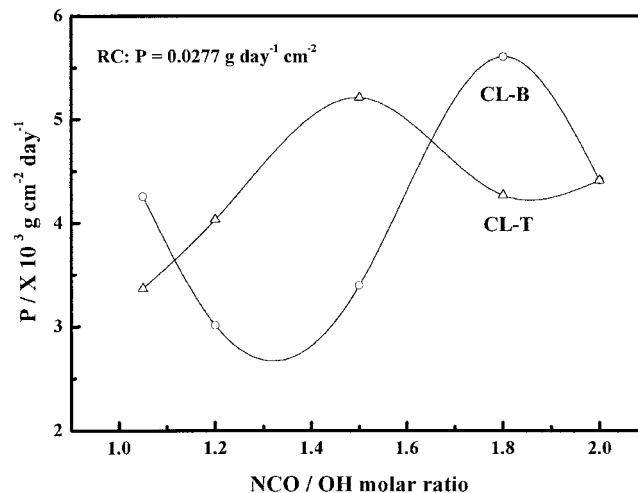**Figure 5** The water resistivity (R) of the RC and coated films.

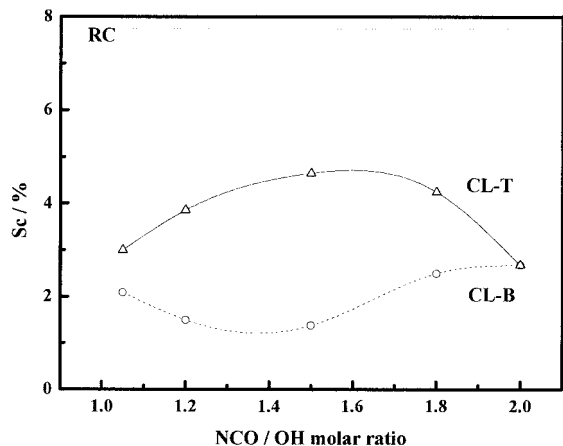**Figure 6** The water vapor permeability (P) of the RC and coated films.

Figure 7 The extent of size contraction (Sc) for the RC and coated films.

Figure 9 TGA curves of the coared films and RC film.

bility of RC film. Simultaneously, the coated films with BDO exhibited more excellent dimensional stability than those with TMP. In addition, the NCO/OH molar ratio in the coatings had a little influence on the size contraction.

Figure 8 shows the percent optical transmittance of RC film, coated films, and corresponding coating in the range of 200 ~ 800 nm. The coated films can fully shade the ultraviolet light in the range of 200 ~ 300 nm due to the effect of polyurethane coating. It is worth noting that transmittance of coated films were higher than that of RC film and corresponding coating in the range of 500~800 nm. Usually, the interface between two dissimilar materials will cause losses in the optical transmission, where the light is scattered
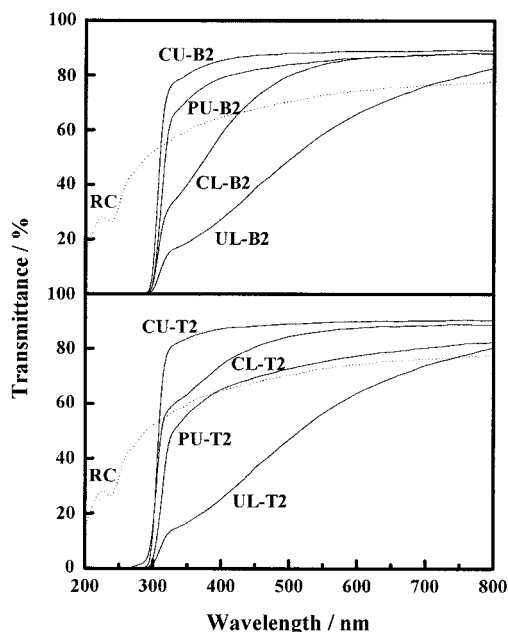
and reflected at the interface of dissimilar solid materials. Thus, the enhancement of transmission of coated films proves that a strong interfacial bonding and a shared network exist between coating layer and RC film. The excellent transmittance reflected a relatively high crosslinking in the interface of the coated films caused by the presence of NL. The crosslink density and the level of the internetwork grafting in the IPNs could enhance their transparent. Interestingly, the transmittance in the range of 300 ~ 400 nm of the coated films with NL was lower than those without NL, as shown in Figure 8. It is well known that lignin has a function in absorbing the ultraviolet light, and thereafter NL kept this characteristic and made the coated films stronger in their ability to resist the ultraviolet light.

Effects of NL in the coatings on properties

Figure 9 shows TGA curves of the coated films and RC film. The decomposition process of RC film was divided into two distinct stages, which were the decomposition in the range of 30 ~ 165°C and the sharp decomposition up to mass residue 0% in the range of 25 ~ 320°C. The decomposition process of the coated films included not only the two stages above, but also the third stage at the beginning of about 325°C. The weight of the coated films remained about 45% in the third stage, which was higher than the 28% of the weight percentage for coating in the coated films. It proved that the chemical reaction and shared networks between cellulose and graft-IPNs coating enhanced thermal stability of the partial cellulose. Simultaneously, the coated films with NL exhibited higher thermal stability than those without NL, especially in the third decomposition stage, suggesting that the coatings containing NL exhibited the more strong adhesion in the interface.

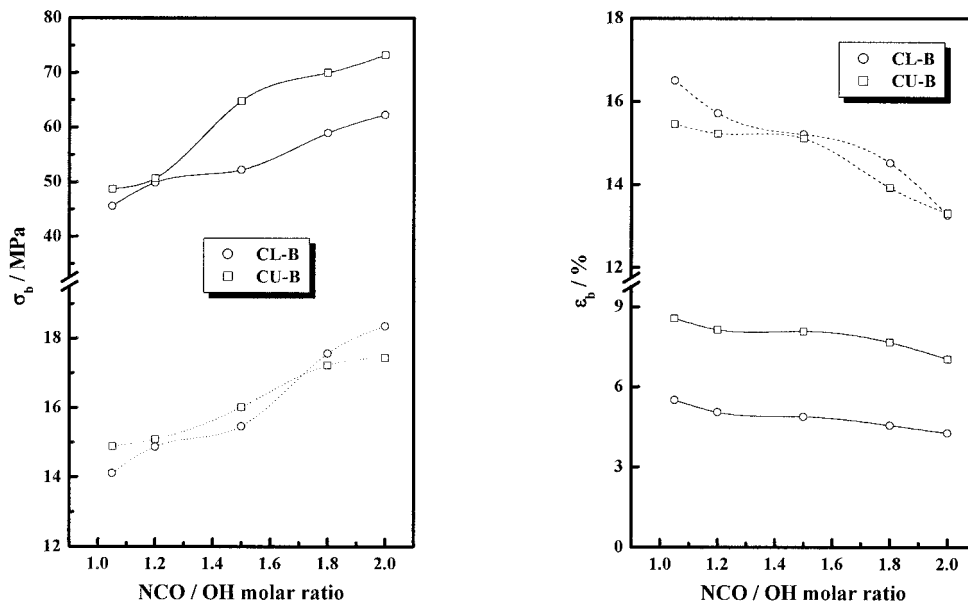Figure 10 showed that CL-B with NL exhibited the inferior mechanical properties (σ_b in the dry and wet

Figure 8 The transmittance plots of the RC and coated films in the range of 200 ~ 800 nm.

Figure 10 The tensile strength and breaking elongation of CL-B and CU-B in dry (—) and wet (· · · ·) states.

state) and higher ε_b in the wet state than CU-B without NL, while Figure 11 showed that the introduction of NL can enhance water resistivity especially at high NCO/OH molar ratios. The introduction of NL enhanced the dense extent of coating layer due to the increase of crosslink density and of the internetwork grafting level. As shown in Figure 12, the extent of size contraction for CL-B with NL was lower than that for CU-B without NL, further suggesting that NL graft-IPNs coating plays a key role in improving the water resistivity and size stability of the films and the interface adhesion.

CONCLUSION

RC films coated with PU and UL coatings exhibited the dense and flat surface, resulting in an enhancement of

dimension stability and a reduction of the water vapor permeability. The formation of shared PU network in the coated films resulted in the enhancement of water resistivity and optical transmittance of the coated films. With an increase of NCO/OH molar ratio, the tensile strength of the coated films increased, but the water resistivity and size contraction hardly changed. The coated films with TMP exhibited the higher breaking elongation at 1.5 of the NCO/OH molar ratio, while those with BDO have relatively high tensile strength, water resistivity, and dimensional stability. The coated films with UL coating containing NL exhibited superior water resistivity and dimensional stability, and can shade the ultraviolet light in the range of 300 ~ 400 nm.
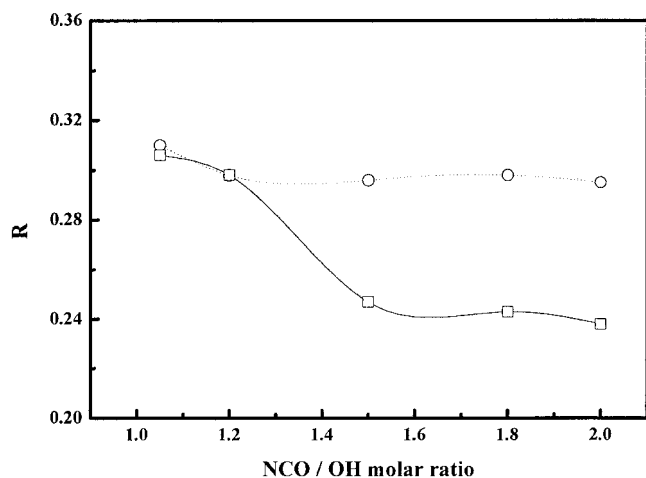
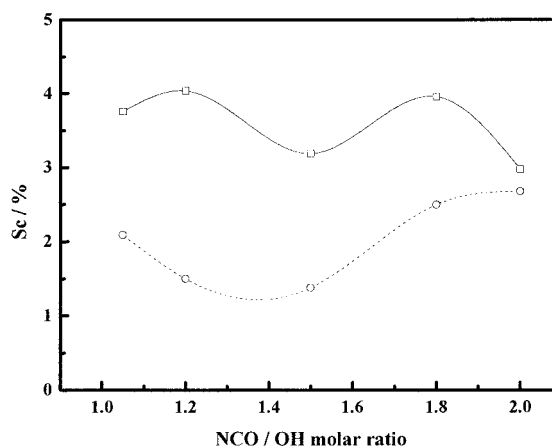**Figure 11** The water resistivity of CL-B (○) and CU-B (□).

Figure 12 The extent of size contraction of CL-B (○) and CU-B (□).

tory of Cellulose and Lignocellulosic Chemistry, Guangzhou Institute of Chemistry, Chinese Academy of Sciences.

References

1. Schuz, J. Prog Polym Sci 1999, 24, 481.
2. Wilkson, S. L. C & E N 2001, 79, 61.
3. Kosokawa, J.; Nishiyama, M. JP 02 127486 (1990).
4. Koseki, H. JP 04 334448 (1992).
5. Hagan, L.; Celeniano, V. D. US 3011910 (1961).
6. Zhang, L.; Zhou, Q. Ind Eng Chem Res 1997, 36, 2651.
7. Liu, H.; Zhang, L. J Appl Polym Sci 2001, 82, 3109.
8. Gong, P.; Zhang, L. Ind Eng Chem Res 1998, 37, 2681.
9. Zhang, L.; Zhou, J.; Huang, J.; Gong, P.; Zhou, Q. Ind Eng Chem Res 1999, 38, 4684.
10. Zhang, L.; Liu, H.; Yan, S.; Yang, G.; Feng, H. J Polym Sci Part B Polym Phys 1997, 35, 2495.
11. Zhang, L.; Huang, J. J Appl Polym Sci 2001, 80, 1213.
12. Zhang, L.; Huang, J. J Appl Polym Sci 2001, 81, 3251.
13. Huang, J.; Zhang, L. Polymer 2002, 43, 2287.
14. Zhang, L.; Ruan, D.; Gao, S. Pat. Appl. CN00128162.3 (Dec. 2000).